Detection of Terahertz Frequencies in S-Doped GaSe Crystals Using Laser Pulses at Telecom Wavelengths

Olesya N. Shevchenko [1,2,*] , Sergey L. Mikerin [3] , Konstantin A. Kokh [4] and Nazar A. Nikolaev [1,2,*]

1   Laboratory of Functional Diagnostics of Low-Dimensional Structures for Nanoelectronics, Novosibirsk State University, Pirogova Str. 2, 630090 Novosibirsk, Russia
2   Terahertz Photonics Group, Institute of Automation and Electrometry, Siberian Branch of the Russian Academy of Sciences, Koptug Ave. 1, 630090 Novosibirsk, Russia
3   Laser Physics Laboratory, Institute of Automation and Electrometry, Siberian Branch of the Russian Academy of Sciences, Koptug Ave. 1, 630090 Novosibirsk, Russia
4   Crystal Growth Laboratory, V.S. Sobolev Institute of Geology and Mineralogy, Siberian Branch of the Russian Academy of Sciences, Koptug Ave. 3, 630090 Novosibirsk, Russia
*   Correspondence: o.shevchenko@nsu.ru (O.N.S.); nazar@iae.nsk.su (N.A.N.)

Abstract: Nonlinear optical crystals of gallium selenide are efficient up- and downconverters of infrared and terahertz frequencies. Their nonlinear properties have been investigated at wavelengths within the main transparency window. However, insufficient attention has been paid to studies at the telecommunication wavelength, especially for sulfur-doped crystals. Closing this gap, we report on the optical and electro-optical properties of $GaSe_{(1-x)}S_x$ crystals (where $x = 0$, 0.03, 0.12, 0.16, and 0.22). For this purpose, the refractive indexes of the ordinary waves at terahertz frequencies and at a wavelength of 1.55 μm have been measured. The detection efficiency of the subterahertz waves in the crystals was studied using Er-fiber laser pulses and compared with that of GaAs, the etalon electro-optical crystal, at this wavelength. This allows us to estimate the dependence of the electro-optic coefficient r_{22} of $GaSe_{(1-x)}S_x$ on the sulfur concentration. It was shown that the sample with $x = 0.12$ has the largest value of the electro-optical coefficient $r_{22} = 1.26$ pm/V and provides the highest detection efficiency among the samples. The potential of employing S-doped GaSe crystals as nonlinear optical converters for photonic devices operating at telecom wavelengths is discussed.

Keywords: terahertz frequencies; millimeter waves; telecommunication wavelength; refractive index; electro-optical coefficient; gallium selenide; GaSe; terahertz time-domain spectroscopy

1. Introduction

Due to the growing need for high data transmission budgets, progress in the development and deployment of optical communication systems has stimulated an increase in carrier and modulation frequencies of transmitted signals up to hundreds of gigahertz [1–3]. The next-generation target range of 120–350 GHz [4,5], which belongs to the so-called millimeter or sub-terahertz (sub-THz) range, is located in the atmosphere's local transparency window and allows unidirectional wireless data transmission for kilometers-long distances [6,7]. Further progress in communication systems will involve the development of the following bands in the vicinity of 667 and 856 GHz [8–10]. The functional abilities of silicon microelectronics drop sharply at such high frequencies [11–13], and it is urgent to search for new materials and methods that will form the basis of next-generation telecommunication devices. We use the term "telecommunication wavelengths" in this paper to refer to the "conventional band" or C-band of fiber optic telecom systems, which lies in the range of 1530–1565 nm (195.9–191.6 THz).

The direct interaction of telecom wavelengths with sub-terahertz (sub-THz) frequencies in a nonlinear optical (NLO) medium is one of the approaches being discussed in the scientific community [14]. It may allow modulation and demodulation of the carrier optical

radiation or even passively outcouple radiofrequencies into free space. The following requirements are presented for the desired NLO media: to be transparent at telecom wavelengths and in the sub-THz range; to have a large nonlinear coefficient; and to be suitable for implementation in planar optical design. The first two requirements are derived from nonlinear optics principles, which state that the efficiency of the interaction of two waves is higher the longer the time of their interaction, that is, the propagation length over which a beneficial energy exchange occurs between them, and the higher the effective nonlinear coefficient of the medium d (which is related to the electro-optical coefficient r as $d \sim n^4 r / 4\pi$, where n is a refractive index at optical wavelength) [15,16].

The most promising in this vein could be binary semiconductor compounds that can be formed into planar structures by molecular beam epitaxy (MBE) or chemical vapor deposition (CVD), such as gallium selenide (GaSe) crystals. The relevance of its application in telecommunication optics is discussed in recent papers [1]. GaSe is often used for NLO devices in the infrared (IR) range [17,18]. It has an absorption coefficient α below 0.03 cm^{-1} at $\lambda \approx 1.5$ μm and less than 1 cm^{-1} in the sub-THz range [19]. GaSe has a large quadratic susceptibility coefficient $d_{22} \approx 54$ pm/V and demonstrates a sufficient laser-induced damage threshold at the level of tens of MW/cm^2 for 10 ns laser pulses [20]. The growth of gallium selenide by MBE methods has been demonstrated in several works [1,21,22]. The disadvantages of the crystal include an extremely low hardness coefficient of ≈ 0 on the Mohs scale and a pronounced splitting orthogonally to the optical axis, which is a cause of defects in the crystal structure and makes it difficult to process mechanically [23]. Doping with isovalent chemical additives, for example, such as S [24–27], Te [25,26,28], Al [25,29–32], and In [27,28,33], is an effective way to improve the mechanical and optical properties of GaSe.

Despite many works aimed at studying the properties of doped and undoped GaSe crystals, a small number of publications are devoted to the results on their linear and nonlinear properties at telecommunication wavelengths.

Only several works are devoted to the study of sulfur-doped GaSe crystals in the optical range [34–37] and in the terahertz range [19,26,38]. None of the works present the refractive index study of sulfur-doped crystals at a wavelength in the vicinity of 1.5 μm. However, there are data from other authors that present the Sellmeer equations obtained from measurements at other wavelengths or from an NLO conversion [39–42].

There are several reports on the generation and detection of THz waves in doped and undoped gallium selenide crystals using laser radiation at various wavelengths, including 0.8 μm [2,3,8,43], 1 μm [9,10], 2 μm [44], and 10 μm [45,46]. However, to the best of our knowledge, crystals have not been studied as NLO generators and detectors of terahertz waves when pumped by laser radiation with wavelengths in the vicinity of 1.5 μm.

We find only two reports on the electro-optical coefficient measurement of the undoped crystals at a wavelength of about 1 μm [47,48].

Thus, seeing the lack of data, we present the study of the linear and nonlinear optical (electro-optical) properties of sulfur-doped gallium selenide crystals. It is done using a terahertz time-domain spectrometer (THz-TDS) configuration, wherein the crystals serve as electro-optic detectors for THz waves probed by radiation from an Er-fiber laser with a wavelength of 1.55 μm. For this purpose, we measure the ordinary refractive index at a wavelength of 1547 nm and in the range of 136–1500 μm (2.2–0.2 THz, respectively) of GaSe$_{(1-x)}$S$_x$ (GaSe:S) crystals, where $x = 0, 0.03, 0.12, 0.16,$ and 0.22. The dispersion of the terahertz refractive index is approximated in the form of the Sellmeier equations, and the coherence lengths L_{coh} providing efficient NLO interaction between telecom and THz waves were calculated. By comparing THz detection efficiency with a high-quality gallium arsenide (GaAs) crystal, the value of the electro-optical coefficients r_{22} of GaSe:S samples was estimated. All the results are compared with the previous studies. The optimum level of doping and the potential of employing GaSe:S crystals as nonlinear optical converters for photonic devices operating at telecom wavelengths is discussed.

2. Samples and Research Methods

GaSe:S crystals were grown from melts using the vertical Bridgman method with thermal field rotation. The detailed description can be found elsewhere [49]. The atomic inclusion of sulfur was determined using an energy-dispersive X-ray spectrometer in combination with a scanning electron microscope. Direct chemical analysis measurements were performed on the cleaved surface of a GaSe:S single crystal, analogous to the work [19] and confirmed by the variation of the absorption edge with relative sulfur content [25]. The samples were cut into two thicknesses: ~1 mm to study the optical properties and ~0.3 mm to measure THz detection efficiency in accordance with the L_{coh} calculated below. The samples were glued into the metal diaphragm, and the surface was then prepared to a high optical quality by exfoliation using adhesive tape. The refractive index of the samples was measured at a wavelength of 1547 nm using a Metricon 2010 system (Metricon, USA). According to the device manual, the absolute measuring error is ± 0.003.

The terahertz refractive index of the samples was measured using a THz-TDS developed at the IA&E SB RAS. It has a bandwidth of 0.1–2.6 THz, with a maximum dynamic range of >70 dB achieved at the frequency of 0.3 THz. The spectral resolution was ~20 GHz. A detailed description of this spectrometer and experimental conditions is given in [50,51].

3. Results

3.1. Refractive Index of GaSe:S in IR and THz Region

The results of measuring the refractive index in the THz spectral range and at λ = 1547 nm are presented in Figures 1 and 2, respectively. It can be seen that as sulfur elements are incorporated into the structure of the GaSe crystal, the value of the refractive index decreases in both ranges.
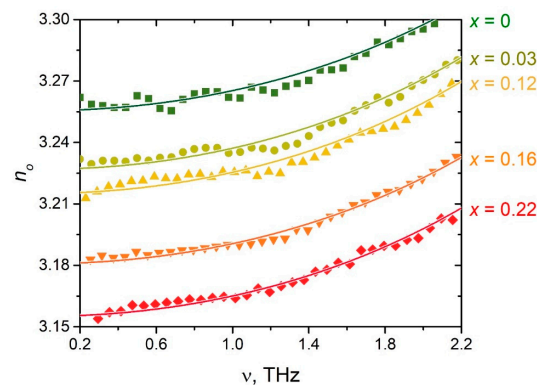

Figure 1. Dispersion of the terahertz refractive index for an ordinary wave of GaSe:S crystal samples. The *x* value is labeled for each curve. Symbols—experimental data, solid curves—approximation by Equation (1).
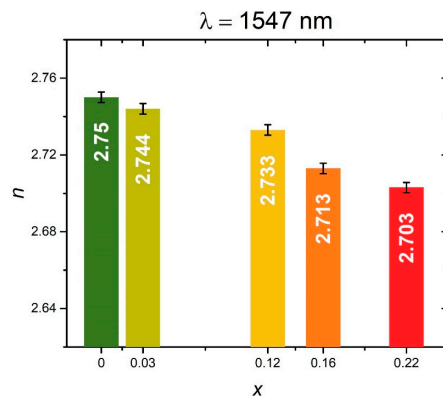

Figure 2. Ordinary refractive index of GaSe:S crystals measured at a wavelength of 1547 nm.

3.2. Calculation of the Crystals' Coherence Length

For the convenience of subsequent calculations, the obtained dispersion curves of the terahertz refractive index were approximated in the form of the Sellmeier equations. The optical properties of the crystal in the far IR range are mainly determined by the phonon mode in the vicinity of 46.7 μm (6.4 THz) [52]. Since the sub-THz range of interest to us is located far enough from this mode, for approximation, it was customary to take the equation in its simplest form:

$$n_o^2 = A + \frac{B\lambda^2}{\lambda^2 - C} \qquad (1)$$

where C is the square of the absorption peak center wavelength in micrometers that determines the dispersion. Since there are no detailed data in the literature on the change in the position of phonons in the vicinity of ~46.7 μm with an increase in the sulfur concentration in the composition of the crystal, in our case it was decided to fix this parameter at the value $C = 46.7^2$ μm$^2 \approx 2266$ μm^2. Coefficients A and B are fitting parameters, the obtained values of which are presented in Table 1.

Table 1. Coefficients of expression (1) for GaSe:S crystals.

x	Coefficient	Value
0	A	8.06
	B	2.54
0.03	A	7.76
	B	2.65
0.12	A	7.70
	B	2.64
0.16	A	7.64
	B	2.48
0.22	A	7.45
	B	2.50

The resulting Sellmeier equations are in good agreement with the data obtained by other authors [41,52–54].

Since the resolution in our measurements is not enough, we deliberately omitted the peak in the vicinity of 0.59 THz from the Sellmeier equation. Its amplitude is rather small, and the bandwidth is quite narrow; thus, it affects the accuracy of the equations only in the range of several tens of GHz around it [2,19]. Moreover, it disappears with an increase in doping concentration [2].

The Equation (2) determines the coherence length, which provides effective NLO interaction of terahertz and femtosecond laser frequencies during crystal propagation [55]:

$$L_{\text{coh}}(\nu_{\text{THz}}) = \frac{c}{2\nu_{\text{THz}}\left(n_{\text{opt}} - \lambda\left.\frac{\mathrm{d}n_{\text{opt}}}{\mathrm{d}\lambda}\right|_{\lambda} - n_{\text{THz}}(\nu_{\text{THz}})\right)}, \qquad (2)$$

where n_{opt} is the refractive index at the wavelength of $\lambda = 1547$ nm (experimental data from Figure 2); $n_{\text{THz}}(\nu)$ is the terahertz refractive index (experimental data from Figure 1); λ is the wavelength of laser radiation; ν_{THz} is the frequency of a terahertz wave. It should be noted that in this case, we consider the simplest case of collinear propagation of laser and THz radiation along the *c*-axis. In our case, the value of $dn_{\text{opt}}/d\lambda$ is not strictly determined since we have not measured the dispersion of the refractive index in the vicinity of $\lambda = 1547$ nm for all crystal compositions. These data are also absent in the literature. Let us assume that with an increase in the sulfur concentration in the crystals, the value and dispersion of the refractive index change smoothly within the values corresponding to the extreme compositions of GaSe and GaS. The parameter $dn_{\text{opt}}/d\lambda$ at $\lambda \approx 1.5$ μm

is equal to $-0.0418\ \mu m^{-1}$ for GaSe and $-0.0292\ \mu m^{-1}$ for GaS [56]. Thus, in the general case, one should expect a deviation of no more than 10% in the denominator of expression (2) for some intermediate value of the sulfur concentration. Taking this into account, for subsequent calculations, we fixed $dn_{opt}/d\lambda = -0.04\ \mu m^{-1}$. Figure 3 depicts the resulting dependences $L_{coh}(\nu_{THz})$. It can be seen that with an increase in the sulfur content, the coherence length increases, which is due to a decrease in the difference between the optical and THz refractive indices. However, the changes in $L_{coh}(\nu_{THz})$ are insignificant and fall within the uncertainty of our calculations due to the aforementioned assumptions.

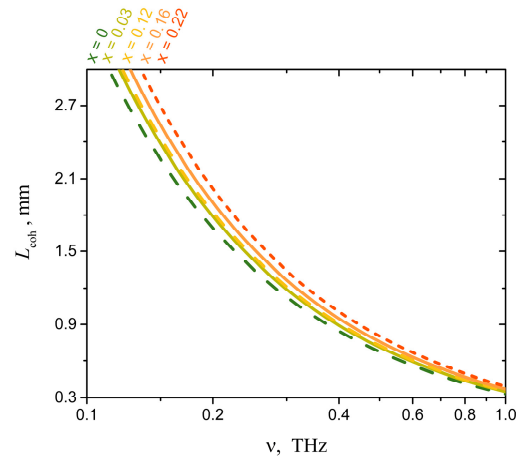**Figure 3.** Coherence length L_{coh} of the interaction of terahertz and laser radiation with a wavelength of λ = 1547 nm in GaSe:S crystals.

At a frequency of 1 THz, the coherence length of crystals with different sulfur concentrations is in the range of $360 \pm 30\ \mu m$ (Table 2). According to this value, all samples were cut from the boules for further study. The actual thickness of the samples is presented in Table 2.

Table 2. Calculated coherence lengths $L_{coh}(\nu = 1\ THz)$ for GaSe:S crystals and measured thicknesses of the prepared samples.

x	L_{coh} (ν = 1 THz), µm	Sample Thickness d, µm
0	329.3	361
0.03	347.5	351
0.12	354.2	342
0.16	370.0	324
0.22	391.5	317

3.3. Detection of THz Radiation in GaSe:S Crystals

3.3.1. Experimental Setup

The study of the detection efficiency in GaSe:S crystal samples was carried out using a specially assembled separate THz-TDS (Figure 4). The source of femtosecond radiation is an erbium fiber laser with λ = 1.55 µm ("Toptica Photonics", Munich, Germany). The pulse width and repetition rate are ~80 fs and ~78 MHz, respectively. The output laser beam with a power of about 220 mW is divided into two parts using a polarizing beam-splitting cube (PBS) for THz generation (90%) and detection (10%). The first one passes through an acoustic-optical modulator (AOM) and is directed to a THz pulse generator represented by a 200-µm-thick p-InAs wafer placed in a magnetic field (B = 0.8 T) of permanent magnets [57]. The generated THz beam is collimated by an off-axis parabolic mirror, passes through a low-pass filter (LPF) that blocks the residual laser radiation, and is focused by a similar parabolic mirror onto the detector electro-optic crystal (EOC). The probing laser beam passes through an optical delay line (ODL), represented by a motorized

linear positioner (8MT173-50-20 from "Standa", Vilnius, Lithuania) with an installed corner-cube retroreflector, and simultaneously with the THz wave, it arrives at the EOC: GaAs, thickness 0.7 mm, with optical anti-reflective coating.
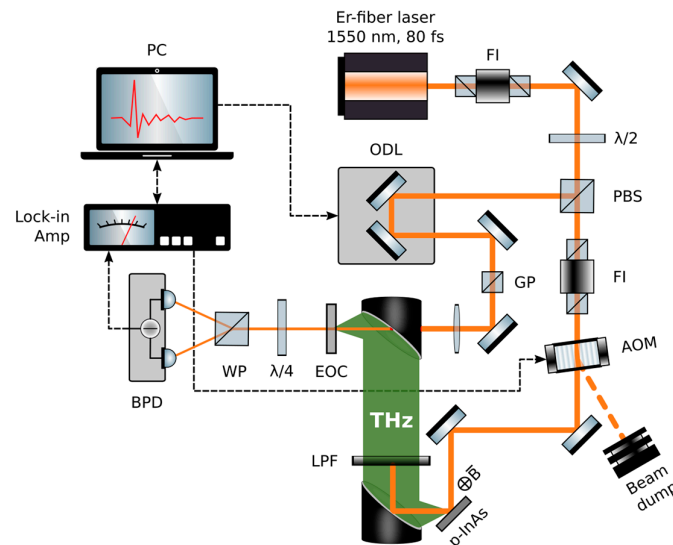

Figure 4. Layout of the experimental setup—terahertz time-domain spectrometer. FI—Faraday isolator, λ/2—half-wave plate, PBS—polarization beamsplitter, ODL—optical delay line, GP—Glan polarizer, AOM—acousto-optical modulator, LPF—low-pass filter, THz—terahertz radiation, EOC—electro-optic crystal, λ/4—quarter-wave plate, WP—Wollaston prism, BPD—balanced photodetector, PC—personal computer.

Detection is carried out by the free-space electro-optic sampling technique based on the Pockels effect [23,58,59]. The change in the polarization of the probe laser beam is measured using a detection system built on a quarter-wave plate, a Wollaston prism (WP), and balance photodetector (BPD). The signal from BPD is fed to a lock-in amplifier (SR844 from "Stanford Research Systems", Sunnyvale, California, USA). It acquire the signal at the modulation frequencies of AOM and THz radiation, respectively. The PC controls the ODL and receives the digital signal from the lock-in amplifier.

3.3.2. The THz Waves Detection Efficiency

After assembling and adjusting the experimental setup, the GaAs crystal detector (Figure 4) was successively replaced by the studied GaSe:S samples, for each of which the spectrometer signal was recorded (Figure 5). As can be seen, the sample with $x = 0.12$ has the highest signal amplitude.
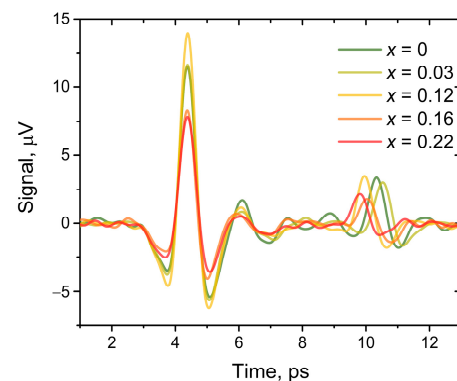

Figure 5. THz waveforms detected with GaSe:S crystals samples.

For clarity, Figure 6 shows the dependence of the peak value of the THz signal amplitude on *x*. The dependence is in good agreement with the work in which a similar study was carried out at the wavelengths of a titanium-sapphire laser [60]. Unfortunately, there were no samples provided with *x* in the range of 0.04 to 0.12; thus, we could not accurately determine the optimal sulfur content for maximum detection efficiency. According to [60], this value *x* should be in the vicinity of 0.11.
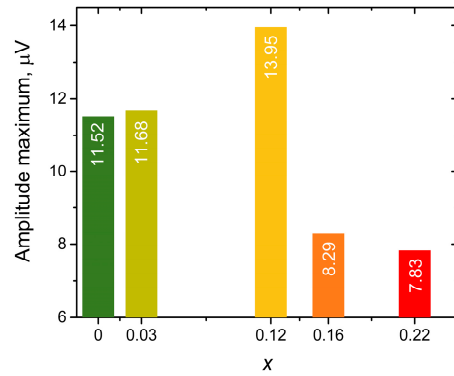

Figure 6. Dependence of the peak amplitude of the THz signal detected with GaSe:S, crystal samples on *x*.

3.3.3. Electro-Optic Coefficient of GaSe:S Samples

Free space electro-optic sampling of THz waves based on the Pockels effect is well described in other works [58,59]. The terahertz field causes a change in the ellipsoid of the refractive indices of the crystal, which leads to the appearance of birefringence, which is detected by the polarization-optical method using a Wollaston prism (WP) and balanced photodetector. WP divides the beam into two parts with mutually orthogonal polarizations I_1 and I_2. Thus, the photodiode currents are:

$$J_1 = s_1 I_1,$$

$$J_2 = s_2 I_2,$$

where s_1 and s_2 are the sensitivities of photodiodes. Taking into account the fact that the photodiodes were manufactured in the same batch, it is permissible to neglect the differences in their sensitivity, i.e., $s_1 = s_2 = s$. In this regard, the current difference is equal to:

$$\Delta J = (I_1 - I_2)s = \Delta I s.$$

The intensity difference recorded by photodiodes is equal to:

$$\Delta I = I_0 \sin \Delta\varphi, \tag{3}$$

where I_0 is the intensity of radiation incident on the detector, $\Delta\varphi$ is the difference between the phase shift of the ordinary and extraordinary waves, which is expressed in terms of:

$$\Delta\varphi = \Delta n \frac{\omega}{c} L, \tag{4}$$

where Δn is the induced birefringence, ω is the frequency of laser radiation, L is the propagation length in an electro-optic medium. The magnitude of $\sin(\Delta\varphi)$ can be estimated as $\sin(\Delta\varphi) \sim \Delta I / I_0$. In our case, measured by the Vega-10A power meter with Ophir head, $I_0 = 12$ mW. ΔI can be calculated using the signal amplitude (Figure 5) and the transimpedance coefficient of the amplifier which is R = 10 k. Thus, $\sin(\Delta\varphi) \sim \Delta I / I_0 = 1.25 \times 10^{-7}$. Then, here and after, we can put $\sin(\Delta\varphi) \sim \Delta\varphi$ for simplicity, as in other works [58,59].

Induced birefringence is expressed in terms of a terahertz field that is applied to the crystal with optimal orientation, through:

$$\Delta n = n_{opt}^3 r E_{THz}, \tag{5}$$

where n_{opt} is the refractive index at the laser wavelength, E_{THz} is the terahertz field, and r is the electro-optic coefficient of the detector crystal.

Combining (4) and (5) preceding expressions yields:

$$\Delta\varphi = \frac{\omega}{c} L n_{opt}^3 E_{THz} r.$$

Thus, the difference in radiation intensities detected by photodiodes is represented by the following expression:

$$\Delta I = I_0 \frac{\omega L n_{opt}^3 E_{THz} r}{c}. \tag{6}$$

Let us take into account the reflection losses from the crystal faces of optical and terahertz waves. In the case of normal incidence on a dielectric surface, we can calculate the optical reflection coefficient using the Fresnel formula:

$$R = \left(\frac{n_1 - n_2}{n_1 + n_2}\right)^2. \tag{7}$$

Considering the amplitude of the THz field, it is necessary to use the amplitude reflection coefficient for these waves:

$$\rho_{THz} = \left(\frac{n_1 - n_2}{n_1 + n_2}\right). \tag{8}$$

Since we only replace the crystal in the system, and the terahertz wave with the probe IR pulse remains the same amplitude and energy, we can compare the electro-optic coefficient of GaSe:S crystals with the well-known one of GaAs. In our case, an antireflection coating with $\lambda = 1.55\ \mu m$ is deposited on the face of the GaAs crystal, thus optical reflection is not considered. Using Equations (6)–(8), we can write:

$$\Delta I_{GaAs} = I_0 \frac{\omega}{c} L_{GaAs} n_{GaAs}^3 E_{THz} \left(1 - \rho_{THz_{GaAs}}\right) r_{GaAs},$$

$$\Delta I_{GaSe} = I_0 \frac{\omega}{c} L_{GaSe} n_{GaSe}^3 E_{THz} \left(1 - \rho_{THz_{GaSe}}\right)(1 - R)^2 r_{GaSe}.$$

Considering E_{THz} is the same in both cases:

$$\frac{\Delta I_{GaAs}}{L_{GaAs} n_{GaAs}^3 r_{GaAs}\left(1 - \rho_{GaAs_{THz}}\right)} = \frac{\Delta I_{GaSe}}{L_{GaSe} n_{GaSe}^3 r_{GaSe}\left(1 - \rho_{GaSe_{THz}}\right)(1 - R)^2}.$$

From here, the electro-optical coefficient for GaSe:S crystals can be expressed as:

$$r_{GaSe} = \frac{\Delta I_{GaSe}}{\Delta I_{GaAs}} \times \frac{L_{GaAs}}{L_{GaSe}} \times \frac{n_{GaAs}^3}{n_{GaSe}^3} \times \frac{\left(1 - \rho_{GaAs_{THz}}\right)}{\left(1 - \rho_{GaSe_{THz}}\right)} \times \frac{1}{(1 - R)^2} \times r_{GaAs}, \tag{9}$$

where L is the corresponding crystal thickness; n_{GaSe}, n_{GaAs} are the refractive indices in the IR range, and R and ρ_{THz} are the optical and terahertz reflection coefficients, respectively.

The values for GaAs are known to be: $r_{GaAs} = r_{41} = 1.5\ pm/V$ [61], $n_{GaAs} = 3.4$ [62], and $n_{GaAs\_THz} = 3.6$ [55]. The values of optical and terahertz refractive indices for GaSe:S crystals are determined by the previously described data (Figures 1 and 2). For simplicity, n_{THz} for GaSe:S crystals are taken at a frequency of 0.3 THz.

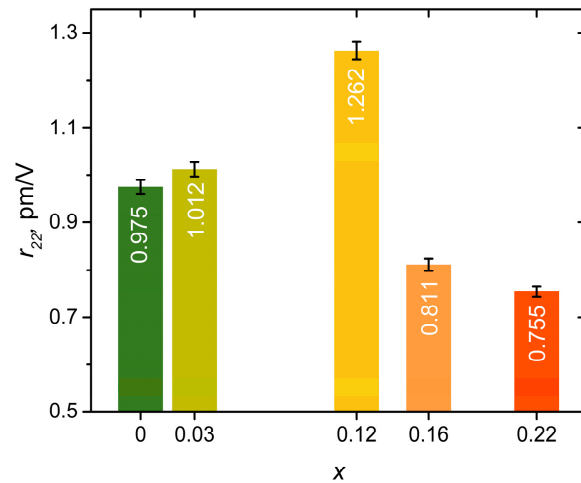The resulting values of $r_{GaSe} = r_{22}$ are shown in Figure 7.

Figure 7. Estimated electro-optic coefficient r_{22} of GaSe:S crystals.

The absolute measurement error of the electro-optical coefficient is estimated to be about 10^{-3} pm/V.

4. Discussions

We compared our results on refractive index measurement of the GaSe:S crystals at a wavelength of 1547 nm and at a frequency of 1 THz with previously published reports. In graphical form, the data are presented in Figures 8 and 9, respectively. The numerical data for λ = 1547 nm are presented in supplementary (Table S1) for convenience. Additionally, it reflects the refractive index measurement technique and the method of crystal growth for each reference, if they were indicated in the article. Ordinary refractive indexes measured in the IR and THz ranges are generally in good agreement with previous work.
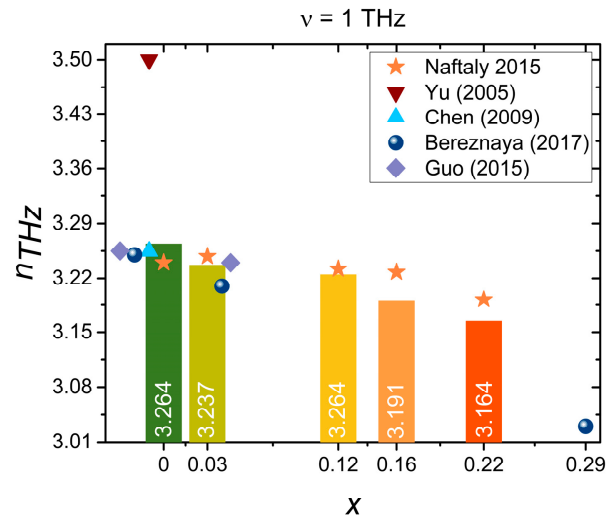

Figure 8. Ordinary refractive index of the GaSe:S crystals at a frequency of 1 THz. Data, measured in this work, are presented in bars and compared with the results published in other works: Guo (2015) [25], Bereznaya (2017) [38], Naftaly (2015) [53], Chen (2009) [54], Yu (2005) [63]. Some data for undoped GaSe is shifted horizontally for better readability.
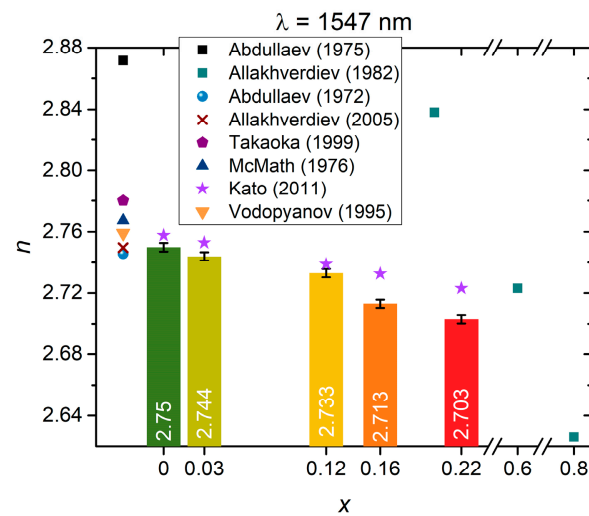
Figure 9. Ordinary refractive index of the GaSe:S crystals at λ = 1547 nm. Data, measured in this work, are presented in bars and compared with the results published in other works: Allakhverdiev (1982) [34], Allakhverdiev (2005) [39], Takaoka (1999) [40], Vodopyanov (1995) [41], Abdullaev (1975) [42], Kato (2011) [56], Abdullaev (1972) [64], McMath (1976) [65]. Some data for undoped GaSe is shifted horizontally for better readability.

In the terahertz range, the value of the ordinary refractive index is in good agreement between most studies. For example, the values for undoped crystals lie in the range from 3.24 to 3.264, which approximately corresponds to an interval of 0.78%. An exception is the work of Yu et al. (2005) [63] in which the refractive index differs significantly from other studies (Figure 8). The authors also report a rather high absorption coefficient for the crystal, which is inconsistent with data from other works in which high-quality crystals were studied. In our case, the crystals also show an extremely low level of absorption for THz waves. The samples in [63] have a high DC conductivity, possibly due to the defects in the crystals. Such conductivity makes a significant contribution to the dielectric susceptibility of the material and, as a consequence, leads to an increase in the refractive index and absorption coefficient at THz frequencies.

Figure 9 shows ordinary refractive index of the GaSe:S crystals at λ = 1547 nm. Since no study has performed direct measurements at this wavelength, the value of the refractive index has been estimated using the suggested in the works Sellmeier equations. It can be seen that the old studies carried out by Abdullaev et al. (1975) [42] and Allakhverdiev et al. (1982) [34] reveal a significant deviation from our results, which may be explained by the imperfection of the crystals due to the limitations of the growth technology at the time. However, in earlier work Abdullaev et al. (1972) [64] report on the refractive index value agrees with our findings. According to the study [42], after a more precise measurement, the authors received results that sharply deviated from the present results. It may also be due to the variation in quality between samples, and the measurement accuracy. Kato and Umemura (2011) [56] proposed to use an effective medium model, based on the values of the refractive indices of pure GaSe and GaS crystals, for estimation of the refractive index of GaSe:S intermediate compounds. From our perspective, the model is effective up to $x = 0.12$. At higher x values, the divergence starts to increase. The reliability of this approach at high sulfur concentrations has to be tested further.

Approbation of GaSe:S crystal samples as detectors of THz waves allowed us to determine the prospects for the use of crystals as nonlinear converters in integrated photonics devices. It ensures the efficient interaction of telecom wavelengths in the vicinity of 1.5 microns and radio frequencies in the sub-terahertz range. Based on the comparison of the detection efficiency of THz waves in the studied samples and the GaAs reference crystal, the electro-optic coefficients of GaSe:S crystals are determined depending on the concentration of sulfur. It is shown that at $x = 0$, the value of the electro-optic coefficient is

r_{22} = 0.975 pm/V, while the crystal with x = 0.12 has r_{22} = 1.262 pm/V and demonstrates the greatest detection efficiency. These data are in good agreement with the values of 1.3 pm/V [47] and 1.1 pm/V [48] obtained at a wavelength of 1.064 micrometers when studying the Pockels effect in undoped GaSe. Our study also confirms that the value of the optimal sulfur concentration x is in the range from 0.04 to 0.12, which is consistent with the results obtained in [66].

Despite having a comparable electro-optical coefficient, GaSe:S has half the coherence length of GaAs. According to the expression (2), this reduces the detection efficiency of THz waves by half. However, GaSe:S is a uniaxial crystal in which the conditions of scalar phase matching are satisfied for the interaction of laser and THz radiation. This means that the optical element can be "tuned" to a certain frequency by the corresponding crystal cut. For example, one can estimate the phase-matching angle similar to [67] for the o–e→o interaction. At a pump wavelength of 1.55 μm and the frequency range of 120–856 GHz indicated in the introduction, the internal phase-matching angle will be 0.155–0.567 degrees.

Phase matching makes it possible to significantly increase the effective length of the nonlinear interaction of optical and THz radiation in the device, for example, from 0.3 to 10 mm using waveguides of the appropriate length, and thus increase the efficiency up to 30 times for frequencies in the vicinity of 1 THz. For even higher frequencies, which may be used in telecom devices of the distant future, the efficiency will be even higher, since the coherence length drops significantly for them. It should be noted that this concept requires the deposition of structures with the required orientation of GaSe:S crystals, but the development of this technology is beyond the scope of this work.

5. Conclusions

In this work, we measured the ordinary refractive index at a wavelength of 1547 nm and in the range of 136–1500 μm (2.2–0.2 THz, respectively) of GaSe$_{(1-x)}$S$_x$ (GaSe:S) crystals, where x = 0, 0.03, 0.12, 0.16, and 0.22. The dispersion of the refractive index in the THz range is in good agreement with previous studies [41,52–54]. The refractive index at λ = 1547 nm is in good agreement with the data presented in modern works [34,39–42,56,64,65]. It is demonstrated that the refractive index consistently reduces in both the near-IR and THz ranges when the sulfur concentrations increase.

We evaluated the electro-optic coefficient of the crystals. It is shown that at x = 0, the value of the electro-optical coefficient is r_{22} = 0.975 pm/V, while the crystal with x = 0.12 has r_{22} = 1.262 pm. The results are in good agreement with the values previously published data at a wavelength of 1.064 microns [47,48].

The results obtained in this work will be useful for accurate estimates of the efficiency of down conversion of the laser frequencies into the terahertz range, for terahertz electro-optic detection systems, as well as for the engineering of modulators for telecommunication wavelengths in the vicinity of 1.55 μm and for the development of nonlinear optical devices for integrated photonics, based on crystals of GaSe doped with sulfur.

Author Contributions: Conceptualization, N.A.N.; Crystal growth, Samples preparation K.A.K.; Investigation, O.N.S. (THz spectroscopy, assembling optical installation, THz detection efficiency measurement, refractive index measurements at 1547 nm), K.A.K. (EDX), S.L.M. (Refractive index measurements at 1547 nm), and N.A.N. (THz spectroscopy); Project administration, N.A.N.; Resources, N.A.N., S.L.M.; Validation, N.A.N., S.L.M.; Writing—original draft, O.N.S.; Writing—review and editing, N.A.N. All authors have read and agreed to the published version of the manuscript.

References

1. Jiang, B.; Hao, Z.; Ji, Y.; Hou, Y.; Yi, R.; Mao, D.; Gan, X.; Zhao, J. High-efficiency second-order nonlinear processes in an optical microfibre assisted by few-layer GaSe. *Light. Sci. Appl.* **2020**, *9*, 63. [CrossRef]
2. Ku, S.A.; Chu, W.-C.; Luo, C.W.; Andreev, Y.; Lanskiy, G.; Shaidukoi, A.; Izaak, T.; Svetlichnyi, V.; Wu, K.-H.; Kobayashi, T. Optimal Te-doping in GaSe for non-linear applications. *Opt. Express* **2012**, *20*, 5029–5037. [CrossRef]
3. Nazarov, M.M.; Sarkisov, S.Y.; Shkurinov, A.; Tolbanov, O.P. Terahertz generation in GaSe0.71S0.29 and GaSe crystals via eee- and eoo-type optical rectification. In Proceedings of the 2012 37th International Conference on Infrared, Millimeter, and Terahertz Waves, Wollongong, Australia, 23–28 September 2012; pp. 1–2. [CrossRef]
4. Saad, W.; Bennis, M.; Chen, M. A Vision of 6G Wireless Systems: Applications, Trends, Technologies, and Open Research Problems. *IEEE Netw.* **2020**, *34*, 134–142. [CrossRef]
5. O'Hara, J.F.; Ekin, S.; Choi, W.; Song, I. A Perspective on Terahertz Next-Generation Wireless Communications. *Technologies* **2019**, *7*, 43. [CrossRef]
6. Jeon, T.-I.; Lehtomäki, J.; Kokkoniemi, J.; Juttula, H.; Mäkynen, A.; Juntti, M. Free Space Loss and Atmospheric Effects. *THz Commun. Paving Way Towards Wirel. Tbps* **2022**, *234*, 51–64. [CrossRef]
7. Kim, G.-R.; Jeon, T.-I.; Grischkowsky, D. 910-m propagation of THz ps pulses through the Atmosphere. *Opt. Express* **2017**, *25*, 25422–25434. [CrossRef]
8. Yamashita, M.; Takahashi, H.; Ouchi, T.; Otani, C. Ultra-broadband terahertz time-domain ellipsometric spectroscopy utilizing GaP and GaSe emitters and an epitaxial layer transferred photoconductive detector. *Appl. Phys. Lett.* **2014**, *104*, 051103. [CrossRef]
9. Shi, W.; Ding, Y.J.; Fernelius, N.; Vodopyanov, K. Efficient, tunable, and coherent 018–527-THz source based on GaSe crystal. *Opt. Lett.* **2002**, *27*, 1454–1456. [CrossRef] [PubMed]
10. Shi, W.; Ding, Y.J.; Fernelius, N.; Hopkins, F.K. Observation of difference-frequency generation by mixing of terahertz and near-infrared laser beams in a GaSe crystal. *Appl. Phys. Lett.* **2006**, *88*, 101101. [CrossRef]
11. Voinigescu, S.P.; Tomkins, A.; Dacquay, E.; Chevalier, P.; Hasch, J.; Chantre, A.; Sautreuil, B. A Study of SiGe HBT Signal Sources in the 220–330-GHz Range. *IEEE J. Solid State Circuits* **2013**, *48*, 2011–2021. [CrossRef]
12. Schroter, M.; Rosenbaum, T.; Chevalier, P.; Heinemann, B.; Voinigescu, S.P.; Preisler, E.; Bock, J.; Mukherjee, A. SiGe HBT Technology: Future Trends and TCAD-Based Roadmap. *Proc. IEEE* **2017**, *105*, 1068–1086. [CrossRef]
13. Hillger, P.; Grzyb, J.; Jain, R.; Pfeiffer, U.R. Terahertz Imaging and Sensing Applications With Silicon-Based Technologies. *IEEE Trans. Terahertz Sci. Technol.* **2019**, *9*, 1–19. [CrossRef]
14. Langrock, C.; Kumar, S.; McGeehan, J.; Willner, A.; Fejer, M. All-optical signal processing using /spl chi//sup (2)/ nonlinearities in guided-wave devices. *J. Light. Technol.* **2006**, *24*, 2579–2592. [CrossRef]
15. Shen, Y.R. *The Principles of Nonlinear Optics*; Wiley-Interscience: New York, NY, USA, 1984.
16. Boyd, R. *Nonlinear Optics*, 4th ed.; Elsevier Science: Amsterdam, The Netherlands, 2020.
17. Singh, N.; Suhre, D.; Balakrishna, V.; Marable, M.; Meyer, R.; Fernelius, N.; Hopkins, F.; Zelmon, D. Far-infrared conversion materials: Gallium selenide for far-infrared conversion applications. *Prog. Cryst. Growth Charact. Mater.* **1998**, *37*, 47–102. [CrossRef]
18. Mason, P.D.; Michaille, L.F. Review of the development of nonlinear materials for mid-IR generation. *Technol. Opt. Countermeas.* **2008**, *7115*, 71150N. [CrossRef]
19. Molloy, J.F.; Naftaly, M.; Andreev, Y.; Kokh, K.; Lanskii, G.; Svetlichnyi, V. Absorption anisotropy in sulfur doped gallium selenide crystals studied by THz-TDS. *Opt. Mater. Express* **2014**, *4*, 2451. [CrossRef]
20. Nikogosyan, D.N. *Nonlinear Optical Crystals: A Complete Survey*; Springer: New York, NY, USA, 2005. [CrossRef]

21. Gan, X.-T.; Zhao, C.-Y.; Hu, S.-Q.; Wang, T.; Song, Y.; Li, J.; Zhao, Q.-H.; Jie, W.-Q.; Zhao, J.-L. Microwatts continuous-wave pumped second harmonic generation in few- and mono-layer GaSe. *Light. Sci. Appl.* **2018**, *7*, 17126. [CrossRef]

22. Jie, W.; Chen, X.; Li, D.; Xie, L.; Hui, Y.Y.; Lau, S.P.; Cui, X.; Hao, J. Layer-Dependent Nonlinear Optical Properties and Stability of Non-Centrosymmetric Modification in Few-Layer GaSe Sheets. *Angew. Chem. Int. Ed.* **2015**, *54*, 1185–1189. [CrossRef]

23. Nahata, A.; Weling, A.S.; Heinz, T.F. A wideband coherent terahertz spectroscopy system using optical rectification and electro-optic sampling. *Appl. Phys. Lett.* **1996**, *69*, 2321–2323. [CrossRef]

24. Huang, C.; Wang, Z.; Ni, Y.; Wu, H.; Chen, S. Experimental and theoretical investigations on the defect and optical properties of S- and Al-doped GaSe crystals. *RSC Adv.* **2017**, *7*, 23486–23493. [CrossRef]

25. Guo, J.; Xie, J.-J.; Li, D.-J.; Yang, G.-L.; Chen, F.; Wang, C.-R.; Zhang, L.-M.; Andreev, Y.M.; Kokh, K.A.; Lanskii, G.V.; et al. Doped GaSe crystals for laser frequency conversion. *Light. Sci. Appl.* **2015**, *4*, e362. [CrossRef]

26. Kang, Z.-H.; Guo, J.; Feng, Z.-S.; Gao, J.-Y.; Xie, J.-J.; Zhang, L.-M.; Atuchin, V.; Andreev, Y.; Lanskii, G.; Shaiduko, A. Tellurium and sulfur doped GaSe for mid-IR applications. *Appl. Phys. B Laser Opt.* **2012**, *108*, 545–552. [CrossRef]

27. Das, S.; Ghosh, C.; Voevodina, O.; Andreev, Y.; Sarkisov, S. Modified GaSe crystal as a parametric frequency converter. *Appl. Phys. B Laser Opt.* **2006**, *82*, 43–46. [CrossRef]

28. Rak, Z.; Mahanti, S.D.; Mandal, K.C.; Fernelius, N.C. Doping dependence of electronic and mechanical properties of GaSe1−xTex and Ga1−xInxSe from first principles. *Phys. Rev. B* **2010**, *82*, 155203. [CrossRef]

29. Zhang, Y.-F.; Wang, R.; Kang, Z.-H.; Qu, L.-L.; Jiang, Y.; Gao, J.-Y.; Andreev, Y.M.; Lanskii, G.V.; Kokh, K.A.; Morozov, A.N.; et al. AgGaS2- and Al-doped GaSe Crystals for IR Applications. *Opt. Commun.* **2011**, *284*, 1677–1681. [CrossRef]

30. Huang, C.; Mao, M.; Wu, H.; Wang, Z.; Ni, Y. Growth and characterization of an Al-doped GaSe crystal. *J. Cryst. Growth* **2018**, *483*, 318–322. [CrossRef]

31. Guo, J.; Xie, J.-J.; Zhang, L.-M.; Li, D.-J.; Yang, G.-L.; Andreev, Y.M.; Kokh, K.A.; Lanskii, G.V.; Shabalina, A.V.; Shaiduko, A.V.; et al. Characterization of Bridgman grown GaSe:Al crystals. *Crystengcomm* **2013**, *15*, 6323–6328. [CrossRef]

32. Guo, J.; Xie, J.-J.; Zhang, L.-M.; Kokh, K.; Andreev, Y.; Izaak, T.; Lanskii, G.; Shaiduko, A.; Svetlichnyi, V.; Andreev, Y. Characterization of optical quality of GaSe:Al crystals by exciton absorption peak parameters. *J. Mater. Sci. Mater. Electron.* **2014**, *25*, 1757–1760. [CrossRef]

33. Singh, N.; Suhre, D.; Rosch, W.; Meyer, R.; Marable, M.; Fernelius, N.; Hopkins, F.; Zelmon, D.; Narayanan, R. Modified GaSe crystals for mid-IR applications. *J. Cryst. Growth* **1999**, *198–199*, 588–592. [CrossRef]

34. Allakhverdiev, K.R.; Guliev, R.I.; Salaev, Y.; Smirnov, V.V. Investigation of linear and nonlinear optical properties of GaS$_x$Se$_{1−x}$crystals. *Sov. J. Quantum Electron.* **1982**, *12*, 947–948. [CrossRef]

35. Wu, C.; Ho, C.; Shen, W.; Cheng, Z.; Huang, Y.; Tiong, K. Optical properties of GaSe1−xSx series layered semiconductors grown by vertical Bridgman method. *Mater. Chem. Phys.* **2004**, *88*, 313–317. [CrossRef]

36. Qasrawi, A.; Gasanly, N. Energy band gap and oscillator parameters of Ga4Se3S single crystals. *Solid State Commun.* **2007**, *142*, 566–568. [CrossRef]

37. Guo, J.; Li, D.-J.; Xie, J.-J.; Zhang, L.-M.; Feng, Z.-S.; Andreev, Y.M.; Kokh, K.A.; Lanskii, G.V.; Potekaev, A.I.; Shaiduko, A.V.; et al. Limiting pump intensity for sulfur-doped gallium selenide crystals. *Laser Phys. Lett.* **2014**, *11*, 55401. [CrossRef]

38. Bereznaya, S.; Korotchenko, Z.; Redkin, R.; Sarkisov, S.Y.; Tolbanov, O.; Trukhin, V.; Gorlenko, N.; Sarkisov, Y.; Atuchin, V.V. Broadband and narrowband terahertz generation and detection in GaSe$_{1−x}$ S$_x$crystals. *J. Opt.* **2017**, *19*, 115503. [CrossRef]

39. Allakhverdiev, K.R.; Baykara, T.; Gulubayov, A.K.; Kaya, A.A.; Goldstein, J.; Fernelius, N.; Hanna, S.; Salaeva, Z. Corrected infrared Sellmeier coefficients for gallium selenide. *J. Appl. Phys.* **2005**, *98*, 093515. [CrossRef]

40. Takaoka, E.T.E.; Kato, K.K.K. Temperature Phase-Matching Properties for Harmonic Generation in GaSe. *Jpn. J. Appl. Phys.* **1999**, *38*, 2755. [CrossRef]

41. Vodopyanov, K.; Kulevskii, L. New dispersion relationships for GaSe in the 0.65–18 μm spectral region. *Opt. Commun.* **1995**, *118*, 375–378. [CrossRef]

42. Abdullaev, G.B.; Allakhverdiev, K.R.; Kulevskiĭ, L.A.; Prokhorov, A.M.; Salaev, E.Y.; Savel'Ev, A.D.; Smirnov, V.V. Parametric conversion of infrared radiation in a GaSe crystal. *Sov. J. Quantum Electron.* **1975**, *5*, 665–668. [CrossRef]

43. Kübler, C.; Huber, R.; Tübel, S.; Leitenstorfer, A. Ultrabroadband detection of multi-terahertz field transients with GaSe electro-optic sensors: Approaching the near infrared. *Appl. Phys. Lett.* **2004**, *85*, 3360–3362. [CrossRef]

44. Yan, D.; Wang, Y.; Xu, D.; Liu, P.; Yan, C.; Shi, J.; Liu, H.; He, Y.; Tang, L.; Feng, J.; et al. High-average-power, high-repetition-rate tunable terahertz difference frequency generation with GaSe crystal pumped by 2 μm dual-wavelength intracavity KTP optical parametric oscillator. *Photonics Res.* **2017**, *5*, 82. [CrossRef]

45. Rao, Z.; Wang, X.; Lu, Y. Tunable terahertz generation from one CO2 laser in a GaSe crystal. *Opt. Commun.* **2011**, *284*, 5472–5474. [CrossRef]

46. Tochitsky, S.Y.; Sung, C.; Trubnick, S.E.; Joshi, C.; Vodopyanov, K.L. High-power tunable, 0.5-3 THz radiation source based on nonlinear difference frequency mixing of CO_2 laser lines. *J. Opt. Soc. Am. B* **2007**, *24*, 2509–2516. [CrossRef]

47. Song, Q.; Chai, L.; Liu, W.; Ma, Q.; Li, Y.; Wang, C.; Hu, M. Measuring effective electro-optic coefficient at 1040 nm by spectral intensity modulation with THz time-domain spectroscopy. *Infrared Phys. Technol.* **2019**, *97*, 54–57. [CrossRef]

48. Cingolani, A.; Ferrara, M.; Lugarà, M.; Levy, F. Pockels effect in gallium selenide. *Solid State Commun.* **1979**, *29*, 677–679. [CrossRef]

49. Kokh, K.; Molloy, J.; Naftaly, M.; Andreev, Y.; Svetlichnyi, V.; Lanskii, G.; Lapin, I.; Izaak, T.; Kokh, A. Growth and optical properties of solid solution crystals GaSe1−xSx. *Mater. Chem. Phys.* **2015**, *154*, 152–157. [CrossRef]

50. Rybak, A.; Antsygin, V.; Mamrashev, A.; Nikolaev, N. Terahertz Optical Properties of KTiOPO4 Crystal in the Temperature Range of (−192)–150 °C. *Crystals* **2021**, *11*, 125. [CrossRef]

51. Wang, C.-R.; Pan, Q.-K.; Chen, F.; Lanskii, G.; Nikolaev, N.; Mamrashev, A.; Andreev, Y.; Meshalkin, A. Phase-matching in KTP crystal for THz wave generation at room temperature and 81 K. *Infrared Phys. Technol.* **2019**, *97*, 1–5. [CrossRef]

52. Chen, C.-W.; Hsu, Y.-K.; Huang, J.Y.; Chang, C.-S.; Zhang, J.-Y.; Pan, C.-L. Generation properties of coherent infrared radiation in the optical absorption region of GaSe crystal. *Opt. Express* **2006**, *14*, 10636–10644. [CrossRef]

53. Naftaly, M.; Molloy, J.F.; Andreev, Y.M.; Kokh, K.A.; Lanskii, G.V.; Svetlichnyi, V.A. Dispersion properties of sulfur doped gallium selenide crystals studied by THz TDS. *Opt. Express* **2015**, *23*, 32820–32834. [CrossRef]

54. Chen, C.-W.; Tang, T.-T.; Lin, S.-H.; Huang, J.Y.; Chang, C.-S.; Chung, P.-K.; Yen, S.-T.; Pan, C.-L. Optical properties and potential applications of ϵ-GaSe at terahertz frequencies. *J. Opt. Soc. Am. B* **2009**, *26*, A58–A65. [CrossRef]

55. Nagai, M.; Tanaka, K.; Ohtake, H.; Bessho, T.; Sugiura, T.; Hirosumi, T.; Yoshida, M. Generation and detection of terahertz radiation by electro-optical process in GaAs using 1.56μm fiber laser pulses. *Appl. Phys. Lett.* **2004**, *85*, 3974–3976. [CrossRef]

56. Kato, K.; Umemura, N. Sellmeier equations for GaS and GaSe and their applications to the nonlinear optics in GaS_xSe_1−x. *Opt. Lett.* **2011**, *36*, 746–747. [CrossRef]

57. Antsygin, V.D.; Mamrashev, A.A.; Nikolaev, N.A.; Potaturkin, O.I. Effect of a Magnetic Field on Wideband Terahertz Generation on the Surface of Semiconductors. *IEEE Trans. Terahertz Sci. Technol.* **2015**, *5*, 673–679. [CrossRef]

58. Planken, P.C.M.; Nienhuys, H.-K.; Bakker, H.J.; Wenckebach, T. Measurement and calculation of the orientation dependence of terahertz pulse detection in ZnTe. *J. Opt. Soc. Am. B* **2001**, *18*, 313–317. [CrossRef]

59. Gallot, G.; Grischkowsky, D. Electro-optic detection of terahertz radiation. *J. Opt. Soc. Am. B* **1999**, *16*, 1204–1212. [CrossRef]

60. Andreev, Y.; Lanskii, G.V.; Kokh, K.A.; Svetlichnyi, V. Optical rectification and down-conversion of fs pulses into mid-IR and THz range in GaSe $_{1-x}$ S $_x$. *Int. Conf. At. Mol. Pulsed Lasers XII* **2015**, *9810*, 98101P. [CrossRef]

61. Madelung, O. *Semiconductors: Data Handbook*, 3rd ed.; Springer: Berlin/Heidelberg, Germany; GmbH: Berlin, Germany, 2004; ISBN 9783642623325.

62. Skauli, T.; Kuo, P.S.; Vodopyanov, K.L.; Pinguet, T.J.; Levi, O.; Eyres, L.A.; Harris, J.S.; Fejer, M.M.; Gerard, B.; Becouarn, L.; et al. Improved dispersion relations for GaAs and applications to nonlinear optics. *J. Appl. Phys.* **2003**, *94*, 6447–6455. [CrossRef]

63. Yu, B.L.; Zeng, F.; Kartazayev, V.; Alfano, R.R.; Mandal, K.C. Terahertz studies of the dielectric response and second-order phonons in a GaSe crystal. *Appl. Phys. Lett.* **2005**, *87*, 182104. [CrossRef]

64. Abdullaev, G.B.; Kulevskii, L.A.; Prokhorov, A.M.; Savel'Ev, A.D.; Salaev, E.Y.; Smirnov, V.V. A New Effective Material for Nonlinear Optics. *J. Exp. Theor. Phys. Lett.* **1972**, *16*, 90.

65. McMath, T.A.; Irwin, J.C. Indices of refraction of GaS and GaSe. *Phys. Status Solidi* **1976**, *38*, 731–738. [CrossRef]

66. Atuchin, V.V.; Andreev, Y.M.; Kokh, K.A.; Lanskii, G.V.; Shaiduko, A.V.; Izaak, T.I.; Svetlichnyi, V.A. Optimal doping of GaSe with isovalent elements. *Nonlinear Opt. Appl. VII* **2013**, *8772*, 234–242. [CrossRef]

67. Liu, K.; Xu, J.; Zhang, X.-C. GaSe crystals for broadband terahertz wave detection. *Appl. Phys. Lett.* **2004**, *85*, 863–865. [CrossRef]